

A DERIVATIVE-FREE MARTINGALE NEURAL NETWORK SOC-MARTNET FOR THE HAMILTON-JACOBI-BELLMAN EQUATIONS IN STOCHASTIC OPTIMAL CONTROLS *

WEI CAI[†], SHUIXIN FANG[‡], WENZHONG ZHANG[§], AND TAO ZHOU[¶]

Abstract. In this paper, we propose an efficient derivative-free version of a martingale neural network SOC-MartNet proposed in *Cai et al.* [2] for solving high-dimensional Hamilton-Jacobi-Bellman (HJB) equations and stochastic optimal control problems (SOCPs) with controls on both drift and volatility. The solution of the HJB equation consists of two steps: (1) finding the optimal control from the value function, and (2) deriving the value function from a linear PDE characterized by the optimal control. The linear PDE is reformulated into a weak form of a new martingale formulation from the original SOC-MartNet where all temporal and spatial derivatives are replaced by an univariate, first-order random finite difference operator approximation, giving the derivative-free version of the SOC-MartNet. Then, the optimal feedback control is identified by minimizing the mean of the value function, thereby avoiding the need for pointwise minimization on the Hamiltonian. Finally, the optimal control and value function are approximated by neural networks trained via adversarial learning using the derivative-free formulation. This method eliminates the reliance on automatic differentiation for computing temporal and spatial derivatives, offering significant efficiency in solving high-dimensional HJB equations and SOCPs.

Key words. Hamilton-Jacobi-Bellman equation; high dimensional PDE; stochastic optimal control; deep neural networks; adversarial networks; martingale formulation.

MSC codes. 49L12, 49L20, 49M05, 65C30, 93E20

1. Introduction. In this paper, we consider the numerical solution of high-dimensional Hamilton-Jacobi-Bellman (HJB)-type equations and their applications to stochastic optimal control problems (SOCPs). The considered HJB equation is given in the form of

$$(1.1) \quad \partial_t v(t, x) + \inf_{\kappa \in U} H(t, x, \kappa, \partial_x v(t, x), \partial_{xx}^2 v(t, x)) = 0, \quad (t, x) \in [0, T) \times \mathbb{R}^d$$

with a terminal condition

$$(1.2) \quad v(T, x) = g(x), \quad x \in \mathbb{R}^d.$$

Here H is the Hamiltonian in form of

$$(1.3) \quad H(t, x, \kappa, z, p) := \frac{1}{2} \text{Tr} (p \bar{\sigma} \bar{\sigma}^\top(t, x, \kappa)) + z^\top \bar{\mu}(t, x, \kappa) + c(t, x, \kappa)$$

*This work of SF and TZ is supported by the NSF of China (under grant 12288201) and the Youth Innovation Promotion Association (CAS). WZ is supported by the Ministry of Science and Technology of China (under grant 2022YFA1005200) and the NSF of China (under grant 1220012530). Date: August 26, 2024.

[†]Department of Mathematics, Southern Methodist University, Dallas, TX 75275, USA. Corresponding author. (cai@smu.edu).

[‡]Institute of Computational Mathematics and Scientific/Engineering Computing, Academy of Mathematics and Systems Science, Chinese Academy of Sciences, Beijing, 100190, P. R. China. Corresponding author. (sxfang@amss.ac.cn).

[§]Suzhou Institute for Advanced Research, University of Science and Technology of China, Suzhou, Jiangsu, 215000, P. R. China. (wenzhong@ustc.edu.cn).

[¶]Institute of Computational Mathematics and Scientific/Engineering Computing, Academy of Mathematics and Systems Science, Chinese Academy of Sciences, Beijing, 100190, P. R. China. Corresponding author. (tzhou@lsec.cc.ac.cn).

for $(t, x, \kappa, z, p) \in [0, T] \times \mathbb{R}^d \times U \times \mathbb{R}^d \times \mathbb{R}^{d \times d}$ with $U \subset \mathbb{R}^m$, where $\bar{\mu}$, $\bar{\sigma}$ and c are given functions valued in \mathbb{R}^d , $\mathbb{R}^{d \times p}$ and \mathbb{R} , respectively. The operators $\partial_x = \nabla_x$ and $\partial_{xx}^2 = \nabla_x \nabla_x^\top$ are the gradient and Hessian operator, respectively.

The Physics-Informed Neural Network (PINN) [4, 6, 7, 11, 12] is a widely used method for solving high-dimensional partial differential equations (PDEs). However, when applied to the HJB equation (1.1), PINN relies on automatic differentiation to compute the Hessian matrix $\partial_{xx}^2 v$, which contains $d \times d$ entries. This approach can become computationally expensive as the spatial dimensionality d increases significantly — a scenario frequently encountered in real-world stochastic optimal control problems with numerous state variables. To address this issue, recently a stochastic dimension gradient decent (SDGD) implementation of PINN was proposed to solve high dimensional PDEs [7].

In this paper, we will attack this problem by proposing a derivative-free version of the martingale neural network SOC-MartNet proposed in [2] for the HJB equation (1.1) where the $\inf_\kappa H$ has no explicit expression and the SDGD PINN will not be applicable. The SOC-MartNet integrated the Varadhan's martingale problem formulation for the HJB equation and dynamics programming, and maximum principle of the verification theory [13] into a deep neural network learning. However, the martingale used there [2] requires the calculation of the Hessian of the value function from the Hamiltonian of the HJB equation, which poses a challenge to extremely high dimensional problems. In this paper, a new martingale will be proposed to avoid all types of spatial derivatives of the value function for a more efficient version of SOC-MartNet. For this purpose, we first use an optimal feedback control function to obtain the linear version of the HJB equation (1.1). Then we introduce a random finite difference operator (RDO) to approximate all the temporal and spatial derivatives in the linear PDE. Here, the RDO is univariate and of first order, and thus enjoys computational efficiency. Then, the linear PDE is solved by an adversarial learning for its weak formulation. Finally, we find the optimal feedback control by minimizing the mean of the value function, instead of the pointwise minimization of the Hamiltonian. Numerical results demonstrate that our method can efficiently solve the high-dimensional HJB equation.

2. Derivative-free formulations.

2.1. Problem reformulation. By inserting (1.3) into the HJB equation (1.1), we can reexpress the latter into

$$(2.1) \quad \partial_t v(t, x) + \inf_{\kappa \in U} \{ \mathcal{L}^\kappa v(t, x) + c(t, x, \kappa) \} = 0, \quad (t, x) \in [0, T] \times \mathbb{R}^d$$

where

$$(2.2) \quad \mathcal{L}^\kappa := \mu^\top(t, x, \kappa) \partial_x + \frac{1}{2} \text{Tr} \{ \sigma \sigma^\top(t, x, \kappa) \partial_{xx}^2 \} \quad \text{for } \kappa \in U.$$

By introducing the optimal feedback control function u defined by

$$(2.3) \quad u(t, x) := \arg \min_{\kappa \in U} \{ \mathcal{L}^\kappa v(t, x) + c(t, x, \kappa) \}, \quad (t, x) \in [0, T] \times \mathbb{R}^d,$$

the HJB equation (2.1) degenerates into a linear PDE as

$$(2.4) \quad (\partial_t + \mathcal{L}^u) v(t, x) + c(t, x, u(t, x)) = 0, \quad (t, x) \in [0, T] \times \mathbb{R}^d$$

with $\mathcal{L}^u := \mathcal{L}^{u(t, x)}$ for convenience. Then the HJB equation (2.1) comes down to find the tuple (u, v) satisfying (2.4) and (2.3), simultaneously.

2.2. Random formulation for 2nd-order derivatives. We first consider a random formulation for the controlled second-order differential operator defined by

$$(2.5) \quad \mathcal{D}_0^u := \partial_t + \mathcal{L}^u = \partial_t + \mu^\top(t, x, u(t, x)) \partial_x + \frac{1}{2} \text{Tr} \{ \sigma \sigma^\top(t, x, u(t, x)) \partial_{xx}^2 \}$$

for $(t, x) \in [0, T] \times \mathbb{R}^d$ and $u \in \mathcal{U}_{\text{ad}}$ with \mathcal{U}_{ad} the set of admissible feedback controls defined by

$$(2.6) \quad \mathcal{U}_{\text{ad}} := \{u : [0, T] \times \mathbb{R}^d \rightarrow U \mid u \text{ is Lebesgue measurable}\}.$$

Let $(\Omega, \mathcal{F}, \mathbb{P})$ be a complete probability space, in which $\zeta : \Omega \rightarrow \mathbb{R}$ is a random variable satisfying

$$(2.7) \quad \mathbb{E}[\zeta] = \mathbb{E}[\zeta^3] = 0, \quad \mathbb{E}[\zeta^2] = 1, \quad \mathbb{E}[\zeta^4] < +\infty.$$

Let $f : \mathbb{R} \rightarrow \mathbb{R}$ be a function smooth at a neighborhood of 0. Then Taylor's expansion leads to

$$\begin{aligned} \mathbb{E}[f(\sqrt{h}\zeta)] - f(0) &= \sqrt{h}f'(0)\mathbb{E}[\zeta] + \frac{h}{2}f''(0)\mathbb{E}[\zeta^2] \\ &\quad + \frac{h^{1.5}}{6}f^{(3)}(0)\mathbb{E}[\zeta^3] + \frac{h^2}{24}\mathbb{E}[f^{(4)}(c\sqrt{h}\zeta)\zeta^4] \\ (2.8) \quad &= \frac{h}{2}f''(0) + O(h^2) \end{aligned}$$

for some $c \in [0, 1]$ following from (2.7).

The expansion (2.8) can be trivially extended to multidimensional cases. Specially, let $g : [0, T] \times \mathbb{R}^d \rightarrow \mathbb{R}$ be a smooth function, and $\xi_h^{t,x}$ be a random vector, which models jumps under controls in \mathbb{R}^d , defined by

$$(2.9) \quad \xi_h^{t,x,u} = \mu(t, x, u(t, x))h + \sigma(t, x, u(t, x))\sqrt{h}W,$$

where $W = (W_1, \dots, W_q)^\top$ is a q -dimensional random vector with its elements W_i independent of each other and satisfying

$$(2.10) \quad \mathbb{E}[W_i] = \mathbb{E}[W_i^3] = 0, \quad \mathbb{E}[|W_i|^2] = 1, \quad \mathbb{E}[|W_i|^4] < \infty, \quad i = 1, 2, \dots, q.$$

Then by the chain rule and (2.8), we have that

$$(2.11) \quad \mathbb{E}[g(t+h, x + \xi_h^{t,x,u})] - g(t, x) = h\mathcal{D}_0^u g(t, x) + O(h^2)$$

with \mathcal{D}_0^u given by (2.5).

Random finite difference operator. Multiplying $1/h$ on both sides of (2.11), we obtain the approximate expression

$$(2.12) \quad \mathbb{E}[\mathcal{D}_h^u g(t, x)] := \mathbb{E}[\mathcal{D}_h^u g(t, x)] = \mathcal{D}_0^u g(t, x) + O(h),$$

where \mathcal{D}_h^u is a random finite difference operator (RDO) defined as

$$(2.13) \quad \mathcal{D}_h^u g(t, x) := \frac{g(t+h, x + \xi_h^{t,x,u}) - g(t, x)}{h}$$

with $\xi_h^{t,x}$ a d -dimensional random vector given by (2.9).

Remark 2.1. The equation (2.12) means that $\mathbb{E}[\mathcal{D}_h^u]$ approximates \mathcal{D}_0^u well for sufficient small h . Moreover, as shown in (2.13), the finite difference operator \mathcal{D}_h^u is not only univariate on $h > 0$, but also of 1st-order one and free of computing any spatial derivatives. This key feature will bring efficiency gains for problems with high spatial dimensionality.

Remark 2.2. An simple example of W satisfying (2.10) can be

$$(2.14) \quad \mathbb{P}(W_i = r) = \mathbb{P}(W_i = -r) := \frac{1}{2r^2}, \quad \mathbb{P}(W_i = 0) := 1 - \frac{1}{r^2}, \quad i = 1, 2, \dots, q$$

with $r > 1$ a hyper parameter. Here the zero outcomes of W_i provide an opportunity to reduce the computation complexity for $\sigma(t, x, u(t, x))W$ in (2.9).

Now we apply the RDO approximation $\mathbb{E}[\mathcal{D}_h^u] \approx \mathcal{D}_0^u = \partial_t + \mathcal{L}^u$ to the linear PDE (2.4), yielding a derivative-free formulation as

$$(2.15) \quad \mathbb{E}[\mathcal{D}_h^u] v(t, x) + c(t, x, u(t, x)) = 0$$

for $(t, x) \in [0, T-h] \times \mathbb{R}^d$, where $\mathbb{E}[\mathcal{D}_h^u]$ is given by (2.12).

2.3. Relation to the martingale neural network SOC-MartNet [2]. The derivative-free formulation (2.15) can also be deduced from a martingale formulation modified from [2]. Specially, for any $(u, v) \in \mathcal{U}_{\text{ad}} \times C_b^{1,2}$, define the cost process $\mathcal{M}^{u,v}$ by

$$(2.16) \quad \mathcal{M}_t^{u,v} := v(t, X_t^u) + \int_0^t c(s, X_s^u, u_s) \, ds, \quad u_t := u(t, X_t^u), \quad t \in [0, T],$$

where $X^u : [0, T] \times \Omega \rightarrow \mathbb{R}^d$ is the state process associated with the HJB equation (2.1), namely,

$$(2.17) \quad X_t^u = x_0 + \int_0^t \mu(s, X_s^u, u_s) \, ds + \int_0^t \sigma(s, X_s^u, u_s) \, dB_s, \quad t \in [0, T],$$

where $\int_0^t \cdot \, dB_s$ denotes the Itô integral with respect to the q -dimensional standard Brownian motion B . Then the Itô formula leads to

$$(2.18) \quad v(t, X_t^u) = v(0, X_0) + \int_0^t \mathcal{D}_0^u v(s, X_s^u) \, ds + \int_0^t \mathcal{D}_1^u v(s, X_s^u) \, dB_s,$$

where \mathcal{D}_0^u is given in (2.5), and $\mathcal{D}_1^u := (\bar{\sigma}^\top(t, x, u(t, x))\partial_x)^\top$. Inserting the above equation into (2.16), we obtain

$$(2.19) \quad \mathcal{M}_t^{u,v} = v(0, X_0^u) + \int_0^t \{\mathcal{D}_0^u v(s, X_s^u) + c(s, X_s^u, u_s)\} \, ds + \int_0^t \mathcal{D}_1^u v(s, X_s^u) \, dB_s.$$

Martingale formulation for PDE (2.4). Under some usual conditions [9, Proposition 1.1.9], if $\mathcal{M}^{u,v}$ is a martingale, i.e.,

$$(2.20) \quad \mathcal{M}_t^{u,v} = \mathbb{E}[\mathcal{M}_T^{u,v} | X_t^u], \quad t \in [0, T],$$

then the drift term on the right side of (2.19) should vanish, that is,

$$(2.21) \quad \partial_t v(t, X_t^u) + \mathcal{L}^u v(t, X_t^u) + c(t, X_t^u, u_t) = 0, \quad (t, \omega) \in [0, T] \times \Omega \text{ a.e.},$$

which means that (2.4) holds for (t, x) explored by X_t^u with positive probability.

For computational implementations, the martingale condition (2.20) is replaced by its discrete version, i.e.,

$$(2.22) \quad \mathbb{E} \left[\Delta \mathcal{M}_{t,h}^{u,v} \middle| X_t^u \right] = 0, \quad t \in [0, T-h],$$

for sufficient small $h > 0$, where

$$(2.23) \quad \Delta \mathcal{M}_{t,h}^{u,v} := v(t+h, X_{t+h}^u) - v(t, X_t^u) + hc(t, X_t^u, u_t),$$

$$(2.24) \quad X_{t+h}^u := X_t^u + \mu(t, X_t^u, u_t)h + \sigma(t, X_t^u, u_t)(B_{t+h} - B_t)$$

obtained by applying the Euler approximation to (2.16) and (2.17), respectively.

The martingale formulation justifies that the linear PDE (2.4) can be solved by enforcing the martingale condition (2.20), which is also derivative-free. Its key point is to encode the derivative $\mathcal{D}_0^u v$ into the dynamic of $t \mapsto v(t, X_t^u)$ as (2.18). This approach is similar to the RDO approach, which encodes $\mathcal{D}_0^u v$ into $h \mapsto v(t+h, x + \xi_h^{t,x,u})$. Actually, the discretized martingale condition (2.22) is equivalent to the RDO formulation (2.15) with W in (2.9) specially taken as

$$(2.25) \quad W \sim \mathcal{N}(0, I_q)$$

with I_q the q -dimensional identity matrix.

To show this, we insert (2.23) and (2.24) into the left side of (2.22) to obtain

$$(2.26) \quad \mathbb{E} \left[\Delta \mathcal{M}_{t,h}^{u,v} \middle| X_t^u = x \right] = \mathbb{E} \left[v(t+h, X_{t+h}^u) \middle| X_t^u = x \right] - v(t, x) + hc(t, x, u(t, x))$$

with $x \in \mathbb{R}^d$. Under (2.25), by comparing (2.9) and (2.24), it holds that

$$\mathbb{E} \left[v(t+h, X_{t+h}^u) \middle| X_t^u = x \right] = \mathbb{E} \left[v(t+h, x + \xi_h^{t,x,u}) \right].$$

Inserting the above equality into (2.26) and using (2.13), we obtain

$$(2.27) \quad \mathbb{E} \left[\Delta \mathcal{M}_{t,h}^{u,v} \middle| X_t^u = x \right] = h \left\{ \mathbb{E} [\mathcal{D}_h^u v(t, x) + c(t, x, u(t, x))] \right\}$$

for $(t, x) \in [0, T-h] \times \mathbb{R}^d$. The above equality means that the RDO approach (2.15) is equivalent to the discrete martingale condition (2.22) localized at $X_t^u = x$.

Remark 2.3. In addition to the martingale approach, the RDO approach (2.15) is introduced because it allows for a broader range of choices for the random vector W in (2.9), beyond the Gaussian one used in (2.24). This flexibility opens up the possibility of extending the RDO approach to fractional PDEs and other applications. Moreover, the derivation of the RDO approach is simpler and does not rely on the Itô calculus, and the resulted formulation (2.15) closely resembles that of the PINN [11]. We believe these features will help readers better understand and apply the method.

2.4. Derivative-free formulation enhanced by Galerkin method. The RDO approach (2.15) and the martingale approach (2.22) can get rid of computing derivatives, but the price lies in the computation of expectationss. It can be quite expansive to compute the pointwise expectation $\mathbb{E} [\mathcal{D}_h^u]$ for each (t, x) , or the conditional expectation $\mathbb{E} [\mathcal{M}_T^{u,v} | X_t^u]$ for each samples of X_t^u . To avoid this issue, we propose to enforce the equality (2.15) in a weak sense such that the expectations can be merged into an inner product with respect to test functions in a Galerkin method.

To be specific, we consider an uncontrolled stochastic process $X : [0, T] \times \Omega \rightarrow \mathbb{R}^d$ to sample the state space \mathbb{R}^d . The distribution of X_s is assumed to be independent of $\xi_h^{t,x,u}$ for any $s \in [0, T]$ and $(t, x) \in [0, T-h] \times \mathbb{R}^d$. Then (2.15) can be enforced in a weak form using a test function $\rho(t, X_t)$ into the following derivative-free formulation:

$$(2.28) \quad \sup_{\rho \in \mathcal{T}} \left| \int_0^{T-h} \mathbb{E} [\rho(t, X_t) \{ \mathbb{E} [\mathcal{D}_h^u] v(t, X_t) + c(t, x, u(t, X_t)) \}] dt \right| = 0,$$

where \mathcal{T} denotes the set of test functions, defined by

$$\mathcal{T} := \{ \rho : [0, T] \times \mathbb{R}^d \rightarrow \mathbb{R} \mid \rho \text{ is smooth and bounded} \},$$

Since $\xi_h^{t,x,u}$ in (2.13) is independent of X_t , we have

$$\mathbb{E} [\mathcal{D}_h^u] v(t, X_t) = \mathbb{E} [\mathcal{D}_h^u v(t, X_t) | X_t]$$

which further implies

$$\begin{aligned} & \mathbb{E} [\rho(t, X_t) \mathbb{E} [\mathcal{D}_h^u] v(t, X_t) + c(t, x, u(t, X_t))] \\ &= \mathbb{E} [\mathbb{E} [\rho(t, X_t) \mathcal{D}_h^u v(t, X_t) + c(t, x, u(t, X_t)) | X_t]] \\ &= \mathbb{E} [\rho(t, X_t) \{ \mathcal{D}_h^u v(t, X_t) + c(t, x, u(t, X_t)) \}]. \end{aligned}$$

The above equation means that we can remove the inner expectation imposed on \mathcal{D}_h^u in (2.28), yielding an equivalent but more computable derivative-free formulation as

$$(2.29) \quad \sup_{\rho \in \mathcal{T}} \left| \int_0^{T-h} \mathbb{E} [\rho(t, X_t) R_h^{u,v}(t, X_t)] dt \right| = 0,$$

where $R_h^{u,v}(t, x)$ is the residual error defined by

$$(2.30) \quad R_h^{u,v}(t, x) := \mathcal{D}_h^u v(t, x) + c(t, x, u(t, x)), \quad (t, x) \in [0, T] \times \mathbb{R}^d,$$

or equivalently,

$$(2.31) \quad R_h^{u,v}(t, x) := h^{-1} \Delta \mathcal{M}_{t,h}^{u,v} \Big|_{X_t^u=x}$$

with $\Delta \mathcal{M}_{t,h}^{u,v}$ given by (2.23) from the martingale approach.

Remark 2.4. (equivalence between SOC-MartNet and WAN [14]) The weak formulation (2.28) can reexpressed as

$$(2.32) \quad \int_0^{T-h} \int_{\mathbb{R}^d} \rho(t, x) \{ \mathbb{E} [\mathcal{D}_h^u] v(t, x) + c(t, x, u(t, x)) \} p(t, x) dt dx = 0, \quad \forall \rho \in \mathcal{T}$$

with $x \mapsto p(t, x)$ the probability density function of the stochastic process X_t . By (2.27) and (2.32), we conclude that the divergence-free martingale neural network SOC-MartNet for solving a semi-linear parabolic equation is equivalent to a weighted Gakerlin-type weak adversarial network (WAN) [14] with the weight being the transitional probability density $p(t, x)$, or a weak form implementation of the PINN [11].

2.5. Derivative-free formulation for HJB equations. Although the linear PDE (2.4) can be solved by enforcing the condition (2.29), the optimal control u is still unknown and need to be solved by combining (2.3). This issue can be addressed by inserting the equality (2.4) to (2.29), which leads to the following derivative-free formulation for the HJB equation (1.1):

(2.33)

$$\min_{(u,v) \in \mathcal{U}_{\text{ad}} \times \mathcal{V}} \int_0^T \mathbb{E}[v(t, X_t)] dt \text{ s.t. } \sup_{\rho \in \mathcal{T}} \int_0^{T-h} \mathbb{E}[\rho(t, X_t) R_h^{u,v}(t, X_t)] dt = 0.$$

for sufficiently small $h > 0$, where \mathcal{U}_{ad} is given by (2.6), and \mathcal{V} is the set of candidate value functions satisfying (1.2), i.e.,

$$(2.34) \quad \mathcal{V} := \{v : [0, T] \times \mathbb{R}^d \rightarrow \mathbb{R} \mid v \in C^{1,2}, v(T, x) = g(x), \forall x \in \mathbb{R}^d\},$$

To show the reasonability of (2.33), we define

$$P(t, x) = \int_0^t p(s, x) ds, \quad (t, x) \in [0, T] \times \mathbb{R}^d,$$

and then use the formula of integration by parts and (1.2) to obtain

$$(2.35) \quad \begin{aligned} \int_0^T \mathbb{E}[v(t, X_t)] dt &= - \int_{\mathbb{R}^d} \int_0^T \partial_t v(t, x) P(t, x) dt dx + \int_{\mathbb{R}^d} g(x) P(T, x) dx \\ &= \int_{\mathbb{R}^d} \int_0^T \{\mathcal{L}^u v(t, x) + c(t, x, u(t, x))\} P(t, x) dt dx \\ &\quad + \int_{\mathbb{R}^d} g(x) P(T, x) dx, \end{aligned}$$

where the second equality follows from (2.4) ensured by the constraint of (2.33); see the deductions in subsection 2.2. Under the equality (2.35), if u , the function of (t, x) , minimizes $\int_0^T \mathbb{E}[v(t, X_t)] dt$, then $u(t, x)$ should also minimize $\mathcal{L}^u v(t, x) + c(t, x, u(t, x))$ for every (t, x) with positive $P(t, x)$, by which the pointwise minimizing condition (2.3) is ensured on the support of P .

2.6. Adversarial learning for the derivative-free SOC-MartNet. The optimization problem can be solved by training deep neural networks with the constraint (2.29) fulfilled by adversarial learning. To this end, we approximate the functions u , v and ρ by the control network $u_\alpha : [0, T] \times \mathbb{R}^d \rightarrow U$, the value network $v_\theta : [0, T] \times \mathbb{R}^d \rightarrow \mathbb{R}$ and the adversarial network $\rho_\eta : [0, T] \times \mathbb{R}^d \rightarrow \mathbb{R}^r$ parameterized by α , θ and η , respectively.

Since the range of u_α should be restricted in the control space U , if $U = [a, b] := \prod_{i=1}^m [a_i, b_i]$ with a_i, b_i the i -th elements of $a, b \in \mathbb{R}^m$, the structure of u_α can be

$$(2.36) \quad u_\alpha(t, x) = a + \frac{b-a}{6} \text{ReLU6}(\psi_\alpha(t, x)), \quad (t, x) \in [0, T] \times \mathbb{R}^d,$$

where $\text{ReLU6}(y) := \min\{\max\{0, y\}, 6\}$ is an activation function and $\psi_\alpha : [0, T] \times \mathbb{R}^d \rightarrow \mathbb{R}^m$ is a neural network with parameter α . Remark 2.5 provides a penalty method to deal with general control spaces.

To fulfill the terminal condition in (2.34), the value network v_θ takes the form of

$$v_\theta(T, x) := g(x), \quad v_\theta(t, x) := \phi_\theta(t, x) \text{ for } t \in [0, T], \quad x \in \mathbb{R}^d,$$

where $\phi_\theta : [0, T] \times \mathbb{R}^d \rightarrow \mathbb{R}$ a neural network parameterized by θ .

The adversarial network ρ_η plays the role of test functions. By our experiment results, ρ_η is not necessarily to be very deep, but instead, it can be a shallow network with enough output dimensionality. A typical example is that

$$(2.37) \quad \rho_\eta(t, x) = \sin(W_1 t + W_2 x + b) \in \mathbb{R}^r, \quad \eta := (W_1, W_2, b) \in \mathbb{R}^r \times \mathbb{R}^{r \times d} \times \mathbb{R}^r$$

for $(t, x) \in [0, T] \times \mathbb{R}^d$, where $\sin(\cdot)$ is the activation function applied on $W_1 t + W_2 x + b$ in an element-wise manner.

Derivative-free SOC-MartNet. Based on (2.33) with $(u_\alpha, v_\theta, \rho_\eta)$ in place of (u, v, ρ) , the solution (u, v) of (2.33) can be approximated by $(u_{\alpha^*}, v_{\theta^*})$ given by

$$(2.38) \quad (\alpha^*, \theta^*) = \lim_{\lambda \rightarrow +\infty} \arg \min_{\alpha, \theta} \left\{ \max_{\eta} L(\alpha, \theta, \eta, \lambda) \right\},$$

where

$$(2.39) \quad L(\alpha, \theta, \eta, \lambda) := \int_0^T \mathbb{E}[v_\theta(t, X_t)] dt + \lambda \left| \int_0^{T-h} \mathbb{E}[\rho_\eta(t, X_t) R_h^{u_\alpha, v_\theta}(t, X_t)] dt \right|^2$$

with $R_h^{u_\alpha, v_\theta}$ given by (2.30).

Remark 2.5. If the control space U is general rather than an interval, the network structure in (2.36) is no longer applicable. This issue can be addressed by appending a new penalty term on the right side of (2.39) to ensure $u_\alpha(t, X_t)$ remains within U . The following new loss function is an example:

$$\bar{L}(\alpha, \theta, \eta, \lambda, \bar{\lambda}) := L(\alpha, \theta, \eta, \lambda) + \bar{\lambda} \int_0^T \mathbb{E}[\text{dist}(u_\alpha(t, X_t), U)] dt,$$

where $L(\alpha, \theta, \eta, \lambda)$ is given in (2.39); $\bar{\lambda} \geq 0$ is a multiplier and $\text{dist}(\kappa, U)$ denotes a certain distance between $\kappa \in \mathbb{R}^m$ and U .

Remark 2.6. Compared with the original SOC-MartNet proposed in [2], the derivative free version (2.38) enjoys the following features:

- The loss function (2.40) and (2.41) are free of computing $\partial_x v$ and $\partial_{xx}^2 v$, where the latter is quite expensive for high-dimensional problems.
- The method can be directly applied to the HJB equation (2.1) with no need of introducing an additional term $\mathcal{L}v(t, x)$ as in (1.1) of [2].
- The random vector W in (2.9) is not necessarily to be Gaussian, which admits sparse outcomes to reduce computation; see Remark 2.2.
- However, the random jumps $\xi_h^{t,x}$ in the random difference operator $\mathcal{D}_h^u v(t, x)$ on the value function in (2.13) depend on the optimal control under approximation, therefore need to be updated along with the optimal control. This implies those jumps can not be pre-calculated before the training as in the original SOC-MartNet.

Mini-batch loss function. For numerical implementations, the mini-batch version of L can be given by

$$(2.40) \quad L(\alpha, \theta, \eta, \lambda; A) := \frac{1}{|A|} \sum_{(n,m) \in A} v_\theta(t_n, X_n^m) \Delta t_n + \lambda |G(\alpha, \theta, \eta; A)|^2,$$

$$(2.41) \quad G(\alpha, \theta, \eta; A) := \frac{1}{|A|} \sum_{(n,m) \in A} \rho_\eta(t_n, X_n^m) R_h^{\alpha, \theta, n, m},$$

Algorithm 2.1 Derivative-free SOC-MartNet for solving the HJB equation (1.1)

Input: I : the maximum number of iterations of stochastic gradient algorithm; M : the total number of sample paths of diffusion process from (3.6); $\delta_1/\delta_2/\delta_3/\delta_4$: learning rates for control network u_α /value network v_θ /adversarial network ρ_η /multiplier λ ; $\bar{\lambda}$: upper bound of multiplier λ ; J/K : number of $(\alpha, \theta)/(\lambda, \eta)$ updates per iteration.

```

1: Initialize the networks  $u_\alpha$ ,  $v_\theta$ ,  $\rho_\eta$  and the multiplier  $\lambda$ 
2: Generate the sample paths  $\{X_n^m\}_{n=0}^N$  of  $X$  for  $m = 1, 2, \dots, M$ .
3: for  $i = 0, 1, \dots, I - 1$  do
4:   Sample the index subset  $A_i \subset \{0, 1, \dots, N - 1\} \times \{1, 2, \dots, M\}$ 
5:   for  $j = 0, 1, \dots, J - 1$  do
6:      $\alpha \leftarrow \alpha - \delta_1 \nabla_\alpha L(\alpha, \theta, \eta, \lambda; A_i)$  //  $L$  is computed by (2.40)
7:      $\theta \leftarrow \theta - \delta_2 \nabla_\theta L(\alpha, \theta, \eta, \lambda; A_i)$ 
8:   end for
9:   for  $k = 0, 1, \dots, K - 1$  do
10:     $\eta \leftarrow \eta + \delta_3 \nabla_\eta L(\alpha, \theta, \eta, \lambda; A_i)$ 
11:     $\lambda \leftarrow \min \{\bar{\lambda}, \lambda + \delta_4 |G(\alpha, \theta, \eta; A_i)|^2\}$  //  $G$  is computed by (2.41)
12:  end for
13: end for

```

Output: u_α and v_θ

where $t_n := nh$, $n = 0, 1, \dots, T/h$, are grid points on $[0, T]$ and

$$R_h^{\alpha, \theta, n, m} := h^{-1} \{v(t_n + h, X_n^m + \xi_h^{n, m, \alpha}) - v(t_n, X_n^m)\} + c(t_n, X_n^m, u_\alpha(t_n, X_n^m))$$

with $(X_n^m, \xi_h^{n, m, \alpha})$, $m = 1, 2, \dots, M$, the independent identically distributed samples of $(X_{t_n}, \xi_h^{t_n, X_{t_n}, u_\alpha})$ given by (2.9), and A is a index subset randomly taken from $\{0, 1, \dots, N - 1\} \times \{1, 2, \dots, M\}$ and is updated at each optimization step. The loss function in (2.40) can be optimized by alternating gradient descent and ascent of $L(\alpha, \theta, \eta, \lambda; A)$ over (α, θ) and (λ, η) , respectively. The details are presented in Algorithm 2.1.

3. Numerical results. We consider the following HJB equation from [1, Section 3.1]:

$$(3.1) \quad \begin{cases} (\partial_t + \Delta_x) v(t, x) + \inf_{\kappa \in \mathbb{R}^d} (2\kappa^\top \partial_x v(t, x) + |\kappa|^2) = 0, & (t, x) \in [0, T) \times \mathbb{R}^d, \\ v(T, x) = 1 + g(x), & x \in \mathbb{R}^d, \end{cases}$$

where the function $g : \mathbb{R}^d \rightarrow \mathbb{R}$ will be specified later. The HJB equation (3.1) is associated with the SOCP:

$$(3.2) \quad u^* = \arg \min_{u \in \mathcal{U}_{\text{ad}}} J(u), \quad J(u) := 1 + \mathbb{E} \left[\int_0^T |u_s|^2 \, ds + g(X_T^u) \right],$$

$$\mathcal{U}_{\text{ad}} = \{u : [0, T] \times \Omega \rightarrow \mathbb{R}^d : u \text{ is } \mathbb{F}^B\text{-adapted}\},$$

$$(3.3) \quad X_t^u = X_0 + \int_0^t 2u_s \, ds + \int_0^t \sqrt{2} \, dB_s, \quad t \in [0, T].$$

The analytic solution to (3.1) is that

$$(3.4) \quad v(t, x) = 1 - \ln \left(\mathbb{E} \left[\exp \left(-g(x + \sqrt{2}B_{T-t}) \right) \right] \right), \quad (t, x) \in [0, T] \times \mathbb{R}^d.$$

To compute the absolute error of numerical solutions, the analytic solution in (3.4) is approximated by the Monte-Carlo method applied on the expectation using 10^6 i.i.d. samples of B_{T-t} .

The numerical method solves $v(0, x)$ for $x \in S_1 \cup S_2$, where S_1 and S_2 are two spatial line segments defined by

$$S_i := \{s\mathbf{e}_i : s \in [-1, 1]\} \quad \text{for } \mathbf{e}_1 := (1, 0, 0, \dots, 0)^\top \in \mathbb{R}^d, \quad \mathbf{e}_2 := (1, 1, \dots, 1)^\top \in \mathbb{R}^d.$$

For an approximation \hat{v} of v , its relative error $R(\hat{v})$ is given by

$$R(\hat{v}) := \frac{\sum_{x \in D_0} |\hat{v}(0, x) - v(0, x)|}{\sum_{x \in D_0} |v(0, x)|},$$

where D_0 consists of M uniformly-spaced grid points on the two line segments S_1 and S_2 , i.e.,

$$(3.5) \quad D_0 = \bigcup_{i=1,2} \bigcup_{j=0}^{M-1} \left\{ \left(\frac{2j}{K-1} - 1 \right) \mathbf{e}_i \right\}.$$

If no otherwise specified, we take $T = 1$ and $N = 100$ for all involved loss functions, and all the loss functions are minimized by the RMSProp algorithm.

In Algorithm 2.1, for each epoch, the sample paths X_n^m for exploration are generated by

$$(3.6) \quad X_{n+1}^m = X_n^m + \mu(t_n, X_n^m, u_n^m) \Delta t_n + \sigma(t_n, X_n^m, u_n^m) (B_{t_{n+1}}^m - B_{t_n}^m)$$

for $m = 1, 2, \dots, M$ and $n = 0, 1, \dots, N-1$, where $B_{t_n}^m$ are the samples of B_{t_n} , and $u_s^m = u_\theta(s, X_n^m)$ with u_θ the control function given by the last epoch. Each point in D_0 are selected as the start point X_0^m of the sample paths in (3.6), i.e., $\{X_0^{(m)} : m = 0, 1, \dots, M\} = D_0$, where $M = 10^4$ is the total number of sample paths in an epoch. At the i -th iteration step, we take the batch size $|M_i|$ of sample paths as $|M_i| = 200, 400, 800$ and 1600 for $i \leq 0.25I, 0.25I < i \leq 0.5I, 0.5I < i \leq 0.75I$ and $0.75I < i \leq I$, respectively, where I denotes the number iteration steps, which is set to 10^3 for $d \leq 500$, and 2×10^3 for $d > 500$.

The learning rates on Lines 6, 7 and 10 of Algorithm 2.1 are set to

$$\delta_1 = \delta_2 = \delta_0 \times 10^{-3} \times 0.01^{i/I}, \quad \delta_3 = 10^{-2} \times 0.01^{i/I}, \quad i = 0, 1, \dots, I-1$$

with $\delta_0 := 3d^{-0.5}$ for $d \leq 1000$ and $\delta_0 := 3d^{-0.8}$ for $d > 1000$. If not otherwise specified, the initial value of λ is 10 with its learning rate $\delta_4 = 10$ and its upper bound $\bar{\lambda}$ set to 10^3 . The inner iteration steps are $J = 2K = 2$. The neural networks u_α and v_θ both consist of 4 hidden layers with $2d + 20$ ReLU units in each hidden layer. The adversarial network ρ_η is given by (2.37) with the output dimensionality $r = 300$.

All the tests are implemented by Python 3.12 and PyTorch 2.4. If no otherwise specified, the algorithm is accelerated by the strategy of Distributed Data Parallel (DDP)¹ on a compute node equipped with 8 GPUs (NVIDIA Tesla V100-SXM2-32GB). When reporting the numerical results, “RE” and “vs” are short for “Relative error” and “versus”, respectively. The term “Mart. Loss” denotes the value of $G(\alpha, \theta, \eta; A)$ defined in (2.41), and “Mean of Value” denotes the value of $1/|A| \sum_{(n,m) \in A} v_\theta(t_n, X_n^m) \Delta t_n$ in (2.40).

¹https://github.com/pytorch/tutorials/blob/main/intermediate_source/ddp_tutorial.rst

3.1. Smooth terminal function. We first consider the HJB equation (3.1) with a smooth terminal function

$$(3.7) \quad g(x) = \ln(0.5(1 + |x|^2)), \quad x \in \mathbb{R}^d.$$

This example is also considered by [1, 3, 5–8, 10, 12]. The numerical results of the derivative-free SOC-MartNet (2.38) are presented in Figure 1, where we can see that our method is accurate and efficient for problem with dimensionality up to 5000.

3.2. Oscillatory terminal function. We turn to consider (3.1) with an oscillatory terminal function as

$$(3.8) \quad g(x) := \frac{1}{d} \sum_{i=1}^d \left\{ \sin(x_i - \frac{\pi}{2}) + \sin((\delta + x_i^2)^{-1}) \right\}, \quad x \in \mathbb{R}^d, \quad \delta = \pi/10.$$

Under (3.8), the true solution along the diagonal of the unite cube, i.e., $s \mapsto v(t, s\mathbf{e}_2)$, is independent of the spatial dimensionality d , whose graphs at $t = 0$ and T are presented in Figure 2. By Figure 2, although $s \mapsto v(T, s\mathbf{e}_2)$ is oscillatory around $s = 0$, the curve of $s \mapsto v(0, s\mathbf{e}_2)$ is relatively smooth and depends on the terminal time T . The relevant numerical results are presented in Figures 3 and 4, where the derivative-free SOC-MartNet still work well for problems with oscillatory terminal conditions and with dimensionality upto 1000.

4. Conclusions. In this paper, a derivative-free form of the martingale neural network SOC-Martnet is proposed for the HJB equation (1.1). The key technique to obtain the derivative-free form is the RDO, which is an univariate and 1st-order operator capable of approximating 2nd-order differential operator. The RDO enjoys high efficiency when applied to weak formulation of linear PDEs. Utilizing this feature, a linear HJB equation obtained using the optimal feedback control can be solved by an adversarial learning with its weak form of a martingale formulation while the RDO approximation gives the derivative-free feature. At the same time, we find the optimal feedback control by minimizing the mean of value function, which avoids pointwise minimization on the Hamiltonian. Numerical results demonstrate the efficiency of our method for solving high-dimensional HJB equations.

REFERENCES

- [1] A. BACHOUCH, C. HURÉ, N. LANGRENÉ, AND H. PHAM, *Deep neural networks algorithms for stochastic control problems on finite horizon: numerical applications*, Methodol. Comput. Appl. Probab., 24 (2022), pp. 143–178.
- [2] W. CAI, S. FANG, AND T. ZHOU, *Soc-martnet: A martingale neural network for the hamilton-jacobi-bellman equation without explicit inf h in stochastic optimal controls*, 2024, <https://arxiv.org/abs/2405.03169>.
- [3] W. E, J. HAN, AND A. JENTZEN, *Deep learning-based numerical methods for high-dimensional parabolic partial differential equations and backward stochastic differential equations*, Commun. Math. Stat., 5 (2017), pp. 349–380.
- [4] Z. GAO, L. YAN, AND T. ZHOU, *Failure-informed adaptive sampling for PINNs*, SIAM J. Sci. Comput., 45 (2023), pp. A1971–A1994.
- [5] J. HAN, A. JENTZEN, AND W. E, *Solving high-dimensional partial differential equations using deep learning*, Proceedings of the National Academy of Sciences, 115 (2018), pp. 8505–8510.
- [6] D. HE, S. LI, W. SHI, X. GAO, J. ZHANG, J. BIAN, L. WANG, AND T.-Y. LIU, *Learning physics-informed neural networks without stacked back-propagation*, in Proceedings of The 26th International Conference on Artificial Intelligence and Statistics, F. Ruiz, J. Dy, and J.-W. van de Meent, eds., vol. 206 of Proceedings of Machine Learning Research, PMLR, 25–27 Apr 2023, pp. 3034–3047.

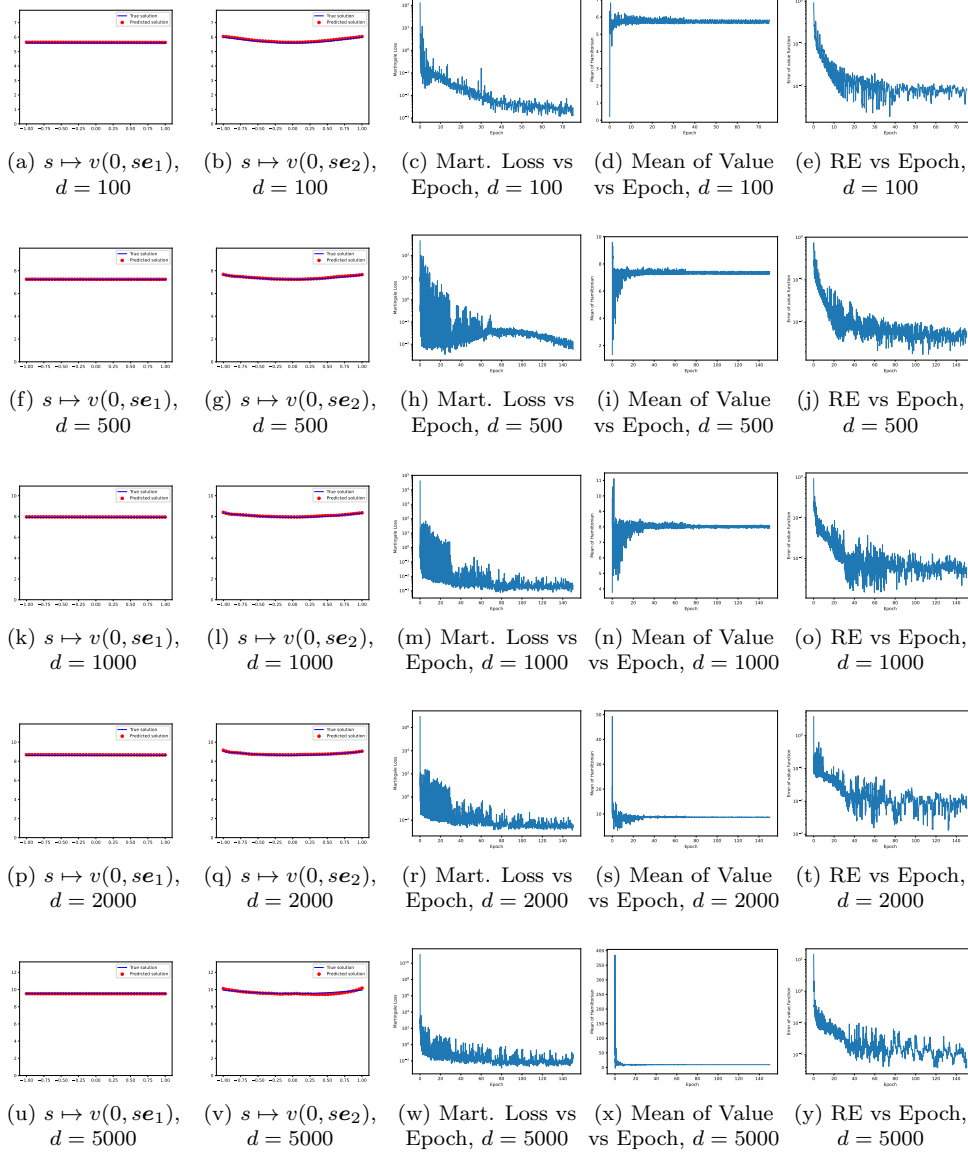


Fig. 1: Numerical results of SOC-MartNet for the HJB equation (3.1) with smooth terminal function (3.7). The running times are 28, 267, 948, 3593 and 21722 seconds for $d = 100, 500, 1000, 2000$ and 5000 , respectively.

- [7] Z. HU, K. SHUKLA, G. E. KARNIADAKIS, AND K. KAWAGUCHI, *Tackling the curse of dimensionality with physics-informed neural networks*, Neural Networks, 176 (2024), p. 106369.
- [8] S. JI, S. PENG, Y. PENG, AND X. ZHANG, *Solving stochastic optimal control problem via stochastic maximum principle with deep learning method*, J. Sci. Comput., 93 (2022), pp. Paper No. 30, 28.
- [9] H. PHAM, *Continuous-time stochastic control and optimization with financial applications*, vol. 61 of Stochastic Modelling and Applied Probability, Springer-Verlag, Berlin, 2009.

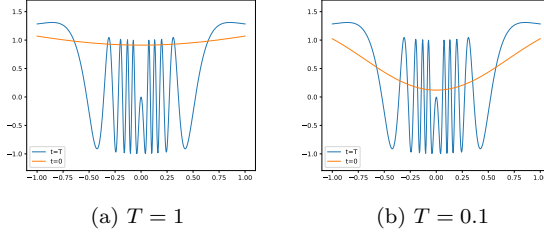


Fig. 2: Graphs of the true solutions $s \mapsto v(t, se_2)$ of the HJB equation (3.1) with a oscillatory terminal function (3.8) and with varying T .

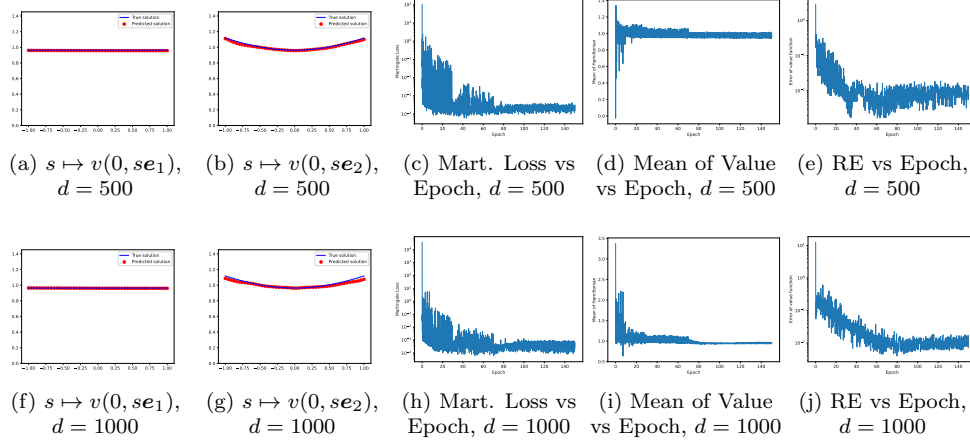


Fig. 3: Numerical results of SOC-MartNet for the HJB equation (3.1) with oscillatory terminal function (3.8) and $T = 1$. The running times are 267 and 949 seconds for $d = 500$ and 1000, respectively.

- [10] M. RAISSI, *Forward-backward stochastic neural networks: Deep learning of high-dimensional partial differential equations*, 2018, [https://arxiv.org/abs/arXiv:1804.07010\[stat.ML\]](https://arxiv.org/abs/arXiv:1804.07010[stat.ML]).
- [11] M. RAISSI, P. PERDIKARIS, AND G. E. KARNIADAKIS, *Physics-informed neural networks: a deep learning framework for solving forward and inverse problems involving nonlinear partial differential equations*, J. Comput. Phys., 378 (2019), pp. 686–707.
- [12] C. WANG, S. LI, D. HE, AND L. WANG, *Is \$l^2\\$ physics informed loss always suitable for training physics informed neural network?*, in *Advances in Neural Information Processing Systems*, A. H. Oh, A. Agarwal, D. Belgrave, and K. Cho, eds., 2022.
- [13] J. YONG AND X. Y. ZHOU, *Stochastic controls*, vol. 43 of *Applications of Mathematics (New York)*, Springer-Verlag, New York, 1999. Hamiltonian systems and HJB equations.
- [14] Y. ZANG, G. BAO, X. YE, AND H. ZHOU, *Weak adversarial networks for high-dimensional partial differential equations*, J. Comput. Phys., 411 (2020), pp. 109409, 14.

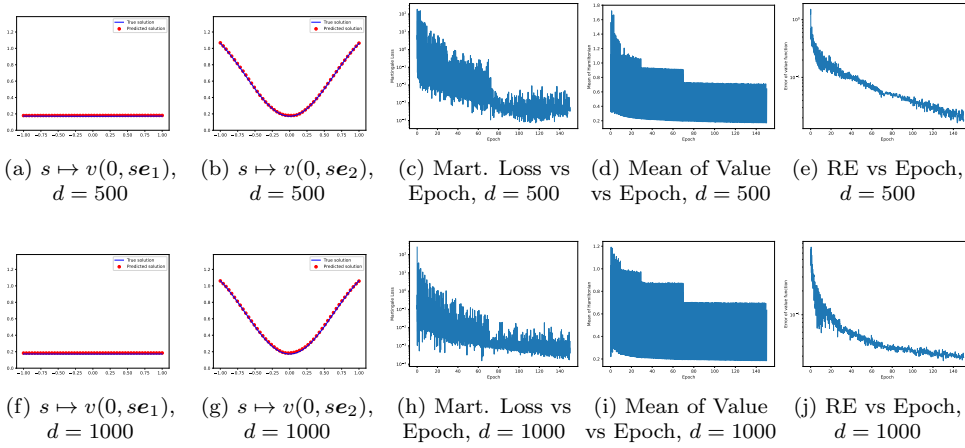


Fig. 4: Numerical results of SOC-MartNet for the HJB equation (3.1) with oscillatory terminal function (3.8) and $T = 0.1$. The running times are 268 and 949 seconds for $d = 500$ and 1000, respectively.